Third-order dispersion compensation for petawatt-level lasers employing object-image-grating self-tiling

2015 Quantum Electron. 45 891

(http://iopscience.iop.org/1063-7818/45/10/891)

Quantum Electronics **45** (10) 891–896 (2015)

CONTROL OF LASER RADIATION PARAMETERS

PACS numbers: 42.55.Rz; 42.60.By; 42.65.Re
DOI: 10.1070/QE2015v045n10ABEH015659

Third-order dispersion compensation for petawatt-level lasers employing object-image-grating self-tiling

Zhaoyang Li, Daxing Rao, Yuxin Leng, Lei Chen, Yaping Dai

Abstract. **A method is proposed for third-order dispersion compensation in compressors of femtosecond petawatt laser facilities employing object-image-grating self-tiling technology to prevent the return of the laser beam in amplifying chains. Simulations are performed for functioning and being developed Nd:glass and Ti:sapphire petawatt-level lasers.**

Keywords: *chirped-pulse amplification, femtosecond pulse compressor with an object-image-grating self-tiling scheme, third-order dispersion.*

1. Introduction

The rapid development of ultra-high power lasers that employ the chirped-pulse amplification (CPA) technique requires large-scale stretchers and compressors [1–3]. The object-image-grating self-tiling (OIGST) method allows the use of meter-sized gratings to compress pulses of existing petawatt-level laser systems [4, 5]. As shown in Fig. 1, the addition of an object-grating and a perpendicularly mounted mirror doubles the effective aperture of the grating while retaining optical efficiency. Unlike conventional compensation tiling [6], OIGST technology is successfully used in femtosecond lasers because it allows one to achieve ideal tiling of the gratings and lacks piston errors of the entire system, which lead to an increase in the output pulse duration [7]. To realise the engineering application of OIGST in a future Chinese multi-petawatt laser facility, our group has recently found that requirements to higher adjustment accuracy and stability within the OIGST method are less strict, compared to the traditional grating tiling method [8]. The first demonstration experiment of laser pulse compression by the OIGST technique has been carried out using our optical parametric chirped-pulse amplification (OPCPA) laser, which allowed us to obtain near-transform-limited pulses with a near-diffraction-limit beam divergence [9]. However, we have also found in this experiment another important potential problem existing in the OIGST CPA laser system which may lead to a damage of an amplifier chain due to the returned reflection pulse (RRP) [8].

The beam path in an OIGST compressor has been described in Refs [4, 9]. As shown in Fig. 1, the input beam is diffracted by the first grating and then by the OIGST tiled grating to the output. During diffraction on the first grating, the beam is broadened in the horizontal plane because of its broad spectrum. Therefore, while the beam is diffracted by the OIGST tiled grating, different spectrum components follow different paths: shorter wavelength components are diffracted by the grating to the output; longer wavelength components are first reflected and then diffracted by the mirror and the grating, respectively, and experience a second mirror reflection to the output. The beam path of two arbitrary spectral components is shown in Fig. 1: the diffraction beam (solid line) on the grating of the OIGST tiled grating is what we need, while the reflection beam (dashed line) accompanies the diffraction beam. If we only focus on the reflection effect, the OIGST tiled grating becomes a standard retro-reflector. Because of the right-angle configuration, the RRP (dashed line) will follow exactly the input path (solid line) and be injected into the amplifier chain. In a petawatt laser system, the slant distance within a grating pair compressor is usually longer than 1.5 m, and accordingly the delay time between the main pulse and the RRP is larger than 10 ns. In an optical parametric amplifier, the pump pulse duration is generally shorter than 10 ns. In this condition, the RRP is not amplified

Zhaoyang Li Shanghai Institute of Optics and Fine Mechanics, Chinese Academy of Sciences, Shanghai 201800, China; Graduate School, China Academy of Engineering Physics, Mianyang 621900, China; School of Electronic and Optical Engineering, Nanjing University of Science and Technology, Nanjing 210094, China; e-mail: zzyylee@siom.ac.cn;
Daxing Rao Shanghai Institute of Laser and Plasma, China Academy of Engineering Physics, Shanghai 201800, China;
Yuxin Leng Shanghai Institute of Optics and Fine Mechanics, Chinese Academy of Sciences, Shanghai 201800, China;
Lei Chen School of Electronic and Optical Engineering, Nanjing University of Science and Technology, Nanjing 210094, China;
Yaping Dai Research Center of Laser Fusion, China Academy of Engineering Physics, Mianyang 621900, China

Received 23 October 2014; revision received 13 November 2014
Kvantovaya Elektronika **45** (10) 891–896 (2015)
Submitted in English

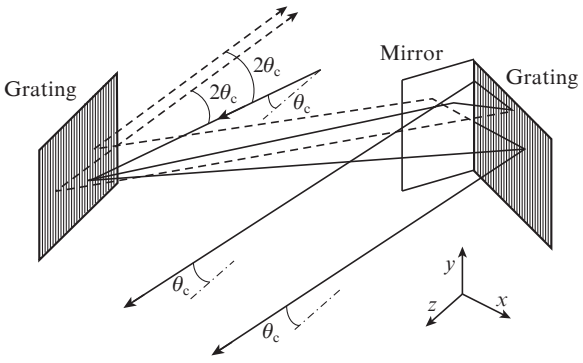

Figure 1. Beam path in an OIGST grating compressor. Solid line and dashed line show direction of diffracted and reflected beams in an OIGST tiled grating, respectively.

and can be suppressed by an optical isolator. Unfortunately, in optical amplifiers of other types (for example, Nd:glass and Ti:sapphire amplifiers), the RRP amplification cannot be avoided.

As shown in Fig. 1, we present in [8] a very simple method to deviate the RRP from the end-window of the amplifier chain by slightly tilting the input beam to the grating groove (y axis) direction with an out-of-plane tilt angle θ_c. However, introducing this out-of-plane tilt angle will change the optical path of the diffraction beam within the parallel grating pair compressor, which will lead to dispersion distortion, and accordingly, to temporal distortion of the compression pulse [10].

In this paper, we have calculated this distortion in Nd:glass and Ti:sapphire lasers and proposed a very simple compensation method. In addition, we present a method for calculating dispersion in an OIGST CPA laser, which could be used to guide the construction of grating-size-limited ultrashort ultra-high laser systems, for example the future femtosecond multi-petawatt laser facility in China.

2. Dispersion distortion

The phase delay ϕ of a laser pulse introduced by a dispersion optical element can be expanded as Taylor series about the centre frequency ω_0 as

$$\phi(\omega) = \phi_0 + \phi'(\omega - \omega_0) + \frac{\phi''}{2}(\omega - \omega_0)^2 + \frac{\phi'''}{6}(\omega - \omega_0)^3 + \frac{\phi''''}{24}(\omega - \omega_0)^4 + \dots, \quad (1)$$

where ϕ_0 is the phase constant; ϕ' is the group delay; ϕ'' is the group-velocity dispersion (GVD); ϕ''' is the third-order dispersion (TOD); and ϕ'''' is the fourth-order dispersion (FOD). Dispersion optical elements in a standard CPA laser system generally include a pulse stretcher, transmission materials (gain media and spatial filter lenses in the amplifier chain) and a pulse compressor. Thus, the condition for the dispersion compensation of a CPA laser system is given by

$$\begin{cases} \mathrm{GVD_s} + \mathrm{GVD_m} + \mathrm{GVD_c} = 0, \\ \mathrm{TOD_s} + \mathrm{TOD_m} + \mathrm{TOD_c} = 0, \\ \mathrm{FOD_s} + \mathrm{FOD_m} + \mathrm{FOD_c} = 0, \\ \dots\dots\dots\dots\dots\dots\dots\dots\dots\dots \end{cases} \quad (2)$$

For GVD, TOD and FOD, the subscripts s, m and c identify the stretcher, transmission materials and compressor.

The main dispersion in a CPA laser system is introduced by the stretcher and the compressor, which have the same optical structure in the form of a parallel grating pair [11, 12]. However, the stretcher has a telescope placed within the grating pair, which introduces opposite-sign dispersion matched to the compressor. The phase delay within a parallel grating pair compressor is given by

$$\phi(\omega) = \frac{\omega}{c}\frac{1 + \cos(\alpha - \beta)}{\cos\theta}\frac{G}{\cos\beta} - \frac{2\pi}{d}G\tan\beta, \quad (3)$$

where α is the angle of incidence; β is the diffraction angle; θ is the out-of-plane tilt angle; G is the perpendicular distance within the grating pair; c is the speed of light; and d is the grating period. Generally, the stretcher and the compressor are designed with same parameters α, G and d, and therefore, the absolute values of $\mathrm{GVD_s}$, $\mathrm{TOD_s}$ and $\mathrm{FOD_s}$ are equal to those of $\mathrm{GVD_c}$, $\mathrm{TOD_c}$ and $\mathrm{FOD_c}$. In this paper, we consider only an aberration-free stretcher configuration [13].

As explained in the Introduction, in order to avoid the potential damage caused by the RRP, an out-of-plane tilt angle is introduced into the compressor. One can see from Fig. 1 that while the input beam is slightly tilted to the y axis, the optical path (as well as the phase delay) of the diffracted laser pulse passing the compressor will deviate from the original one, which will lead to dispersion distortion and break the dispersion balance of the whole CPA system. To introduce the same out-of-plane tilt angle to the stretcher maybe an efficient solution, but which will challenge the multi-pass configuration of the stretcher.

3. Compensation solution

3.1. Nd:glass system

Due to a limited gain bandwidth but a large physical aperture of the Nd:glass, this system could support a sub-picosecond kilo-joule laser pulse. The simulation is performed for our petawatt facility [14] whose structure is given in Fig. 2. A 230-fs, 0.5-nJ seed pulse centred at 1053 nm from the oscillator is stretched to 3 ns by an 8-pass single-grating stretcher, amplified to 400 J by the Nd:glass amplifier chain, and finally re-compressed to around a 400-fs, 350-J pulse by a four-grating single-pass compressor. The duration broadening of the final pulse compared with the seed one is caused by the limited gain bandwidth and nonlinear phase distortions (B-integral) in the amplifier chain, which are 20 nm and 1.7, respectively. The total length of Nd:glass and BK7 lenses in the system is 3.35 m and 0.36 m, respectively. The stretcher and the compressor are designed with the same grating density of 1740 lines $\mathrm{mm^{-1}}$ and the same incident angle of 70°. To compensate for the total GVD of the system, the distance between the gratings is chosen to be 0.4980 and 1.9926 m, respectively. The uncompensated TOD is relatively small, which will not distort the shape of the output sub-picosecond pulse.

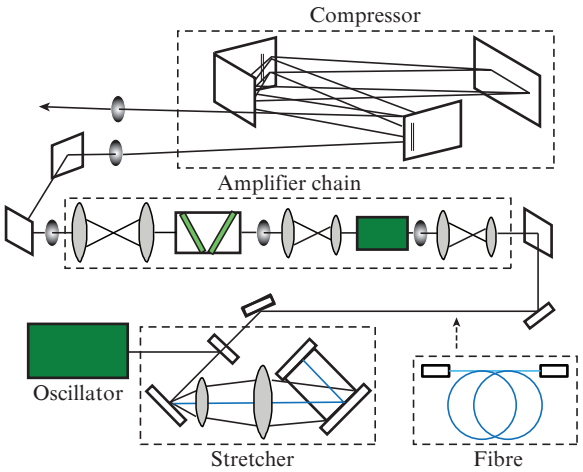

Figure 2. Schematic view of the petawatt Nd:glass facility. The incident beam at the compressor is tilted to avoid coupling of the RRP into the amplifier chain. Fibre is inserted for TOD compensation.

Table 1. GVD, TOD and FOD in a Nd : glass system.

Dispersion element	Dispersion length/m	GVD/fs^2	TOD/fs^3	FOD/fs^4
Stretcher	0.4980×8	2.7150×10^8	-4.11320×10^9	1.0371×10^{11}
Nd : glass	3.35	8.0239×10^4	1.3643×10^5	-1.4924×10^5
BK7 lens	0.36	8.3628×10^3	1.7126×10^4	-2.0547×10^4
Compressor ($\theta_c = 0$)	1.9926×2	-2.7158×10^8	4.1146×10^9	-1.0375×10^{11}
Total system ($\theta_c = 0$)		0	1.5536×10^6	-4.0170×10^7
Compressor ($\theta_c = 1°$)	2.0003×2	-2.7158×10^8	4.1039×10^9	-1.0321×10^{11}
Total system ($\theta_c = 1°$)		0	-9.1464×10^6	4.9983×10^8
Compressor ($\theta_c = 2°$)	2.0236×2	-2.7158×10^8	4.0712×10^9	-1.0156×10^{11}
Total system ($\theta_c = 2°$)		0	-4.1846×10^7	2.1498×10^9
Compressor ($\theta_c = 3°$)	2.0638×2	-2.7158×10^8	4.0151×10^9	-9.8726×10^{10}
Total system ($\theta_c = 3°$)		0	-9.7946×10^7	4.9838×10^9
Silica fibre	0.001	17.263	43.202	−56.899

The GVD, TOD and FOD of dispersion elements within this system are presented in Table 1, which shows that with increasing out-of-plane tilt angle θ_c the dispersion length of the compressor should be increased to compensate for the residual GVD of the system. However, the residual TOD and FOD cannot be compensated, simultaneously. The influence of FOD in a sub-piscosecond pulse can be ignored, and then in this section we only focus on the TOD compensation.

Figure 3a shows the dependences of GVD and TOD/GVD on the out-of-plane tilt angle. The absolute values of GVD and TOD decrease with increasing out-of-plane tilt angle, TOD decreasing faster than |GVD|. The decrease of the compressor |GVD| leads to a residual of the stretcher GVD, which will stretch the duration of the output pulse. In our system, out-of-plane tilt angles of 1° and 2° lead to around 7 and 29-ps pulse stretching, respectively. This GVD distortion can be conveniently eliminated by slightly increasing the dispersion length G_c of the compressor. At the same time, this does not lead to TOD compensation, which deteriorates both the peak intensity and the temporal contrast. Generally, in this case, an extra adjustment of the compressor incident angle α_c is needed. The compensation of GVD and TOD can be obtained simultaneously by adjusting both the dispersion length G_c and the incident angle α_c of the compressor [15]: The dispersion length determines the amount of GVD, TOD and FOD, and the incident angle affects the ratio among GVD, TOD and FOD.

The incident angle α_c and the dispersion length G_c of the compressor can be easily calculated and achieved in the absence of the out-of-plane tilt angle θ_c. However, when an out-of-plane tilt angle is introduced, the incident angle as well as the dispersion length should be adjusted accordingly.

Figure 3b shows the peak intensity of the GVD compensated pulse as a function of the incident angle adjustment at different out-of-plane tilt angles. The highest peak intensities (the TOD compensation) are achieved at incident angle adjustments of 0, −0.04°, −0.20° and −0.46° for $\theta_c = 0$, 1°, 2° and 3°, respectively. One can also see from the figure that in the absence of the incident angle adjustment, the peak intensity of the GVD compensated pulse will decrease rapidly with increasing out-of-plane tilt angle θ_c. Although decreasing the incident angle of the compressor could compensate for the TOD distortion, it may lead to another important problem: the insertion of the second grating into the incident beam, which will destroy the optical arrangement of the compressor.

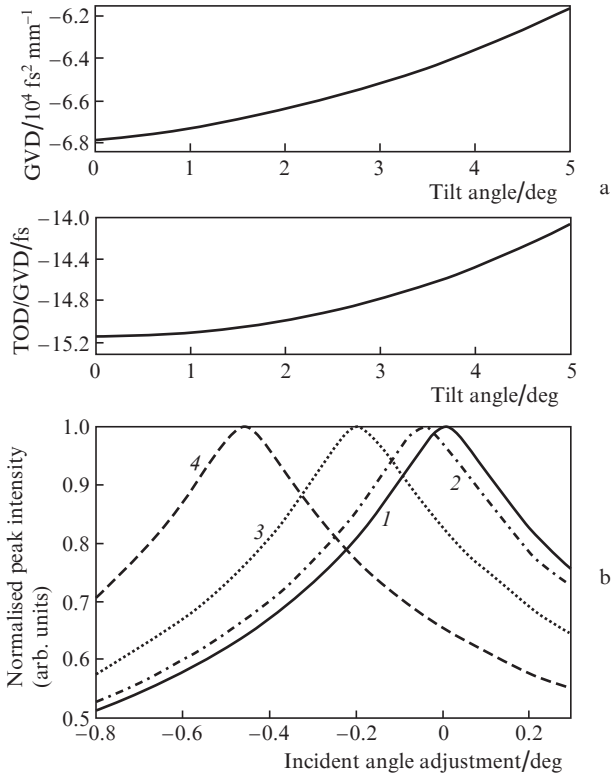

Figure 3. (a) Compressor GVD and TOD/GVD vs. out-of-plane tilt angle θ_c and (b) normalised peak intensity of a GVD compensated pulse vs. incident angle adjustment at θ_c = (*1*) 0, (*2*) 1°, (*3*) 2° and (*4*) 3°.

Besides, the adjustment of the incident angle for a single-pass four-grating compressor is a challenging engineering problem, which requires the precision positioning of meter-sized gratings.

Actually, introducing a prism-pair and grating-pair hybrid configuration into the system is another solution to the TOD compensation [16]. However, this method will aggravate the complexity of a facility and reduce its engineering reliability, especially for a petawatt-level large-scale laser system.

Let us consider a simpler method for the TOD compensation. The negative TOD of the stretcher can be compensated for by using an element with a positive TOD. To this end, use can be made of silica fibre, which has a positive GVD and a

positive TOD (see Table 1). Once a short piece of fibre is introduced into the system, the dispersion compensation condition of the system can be rewritten as

$$\begin{cases} \mathrm{GVD_s} + \mathrm{GVD_f} + \mathrm{GVD_m} + \mathrm{GVD_c} = 0, \\ \mathrm{TOD_c} + \mathrm{TOD_f} + \mathrm{TOD_m} + \mathrm{TOD_c} = 0, \end{cases} \quad (4)$$

where the subscript f identifies the inserted fibre. According to Eqn (4), the TOD-free pulse can be achieved by using a length-optimised silica fibre, whereas the dispersion length G_c (or the perpendicular distance) of the compressor should be adjusted slightly. In this case, the incident angle α_c does not need to be adjusted any more. The optimised fibre length L_f and the corresponding dispersion length G_c of the compressor are given in Table 2.

Table 2. Dispersion length of fibre (L_f) and compressor (G_c) at different out-of-plane tilt angles.

θ_c /deg	L_f/m	G_c/m
0	0	1.9926
1	30.29	2.0041
2	138.57	2.0415
3	328.47	2.1069

The use of silica fibre balances GVD and TOD of the whole system, but brings a new problem: self-phase modulation (SPM). Actually, silica fibre can be treated as another stretcher, and then there are two available two-stage-stretcher configurations: the fibre-grating (FG) configuration and the grating-fibre (GF) configuration. In the FG configuration, a high-energy short pulse from the oscillator is directly coupled into the fibre-stretcher and then the grating-stretcher; therefore, SPM in the fibre-stretcher is a serious problem. However, in the GF configuration, the laser intensity in the fibre-stretcher is reduced by around 13000 times due to a deep chirped pulse by the front grating-stretcher, and thereby the influence of SPM may be negligible.

Normalised and relative intensity profiles of compressed pulses, based on a 6-μm core diameter single-mode fibre (SMF), are presented in Fig. 4. For an out-of-plane tilt angle $\theta_c = 1°$, a 30.29-m-long silica fibre is inserted for dispersion compensation. At $\theta_c = 2°$, use should be made of a 138.57-m-long fibre. In the FG configuration, SPM broadens the pulse spectrum, and part of intensity transfers to spectral components located away from the gain bandwidth of the Nd:glass, which decreases the peak intensity (Fig. 4a). Besides, as shown in Fig. 4b, SPM also deteriorates the temporal contrast. Consequently, the GF configuration becomes the only feasible scheme. At $\theta_c = 2°$, the distortion of the peak intensity and pulse duration is not distinct. Compared with the simulation result in the FG configuration, the degradation of the temporal contrast is very small, and a 10^{-16} temporal contrast 10 ps before the pulse peak can be obtained. In our facility, the beam aperture is 320 mm, and the beam path from the final amplifier to the compressor is around 15 m. Thereby, one should use the out-of-plane tilt angle $\theta_c = 1.5°$ and a 75-m-long silica fibre.

3.2. Ti:sapphire system

The Ti:sapphire laser system could support a femtosecond pulse due to a wide gain bandwidth, but its output energy is limited by a small physical size of the Ti:sapphire crystal.

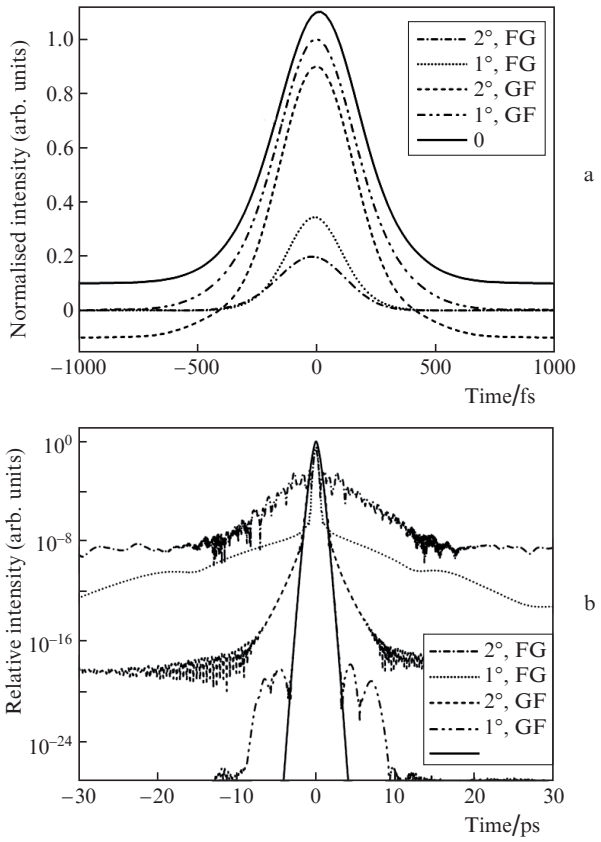

Figure 4. (a) Normalised and (b) relative intensities as functions of time at $\theta_c = 0$, 1° and 2° for configuration in which fibre is located behind the stretcher (GF) and in front of the stretcher (FG). Solid curves correspond to total dispersion compensation at a zero out-of-plane tilt angle.

We performed simulations for on our planned multi-petawatt facility, which is based on two meter-sized golden coated diffraction gratings. A 20-fs seed pulse centred at 800 nm will be stretched to 2 ns, amplified to an energy of ~100 J and finally re-compressed to around 40 fs. The stretcher will have an Offner four-pass single-grating configuration. The grating density, the incident angle and the equivalent grating pair perpendicular distance are chosen to be 1740 lines mm^{-1}, 55° and 0.4263 m, respectively. The *B*-integral of the system is estimated to be around 0.8. The total length of Ti:sapphire and DKDP crystals and BK7 lenses is 1.86, 0.86 and 0.19 m, respectively. The designed GVD, TOD and FOD of the dispersion elements within the system are given in Table 3.

In absence of material dispersion, a dispersion-free pulse will be produced by a stretcher-matched compressor. However, the influence of material dispersion, especially TOD and FOD, on the compressed pulse in a femtosecond system is much more serious than that in a picosecond system. As illustrated above, GVD and TOD for a Nd:glass system can be compensated for simultaneously by adjusting the dispersion length G_c and the incident angle α_c of the compressor. Thus, we have designed a two-pass two-grating compressor configuration. The grating density is 1740 lines mm^{-1}, the incident angle is 56.07° and the grating pair perpendicular distance is 0.8909 m. As shown in Table 3, the compressor could compensate for GVD introduced by front elements, and small amount of TOD is left for reaching the highest peak intensity by compensating the residual FOD.

Table 3. GVD, TOD and FOD for a Ti:sapphire system.

Dispersion element	Dispersion length/m	GVD/fs^2	TOD/fs^3	FOD/fs^4
Stretcher	0.4263×4	8.4883×10^6	-2.3635×10^7	1.0744×10^8
Ti:sapphire crystal	1.86	1.1042×10^5	7.7610×10^4	-2.6624×10^4
DKDP crystal	0.86	3.0327×10^4	3.2025×10^4	-1.8302×10^4
BK7 lens	0.19	8.4721×10^3	6.0867×10^3	-2.0083×10^3
Compressor ($\alpha_c = 56.07°$)	0.8909×2	-8.6375×10^6	2.3585×10^7	-1.0521×10^8
Total system ($\alpha_c = 56.07°$)		0	6.5652×10^4	2.1846×10^6
Compressor ($\theta_c = 6.26°$)	0.8920×2	-8.6375×10^6	2.3583×10^7	-1.0502×10^8
Total system ($\theta_c = 6.26°$)		0	6.3722×10^4	2.3731×10^6

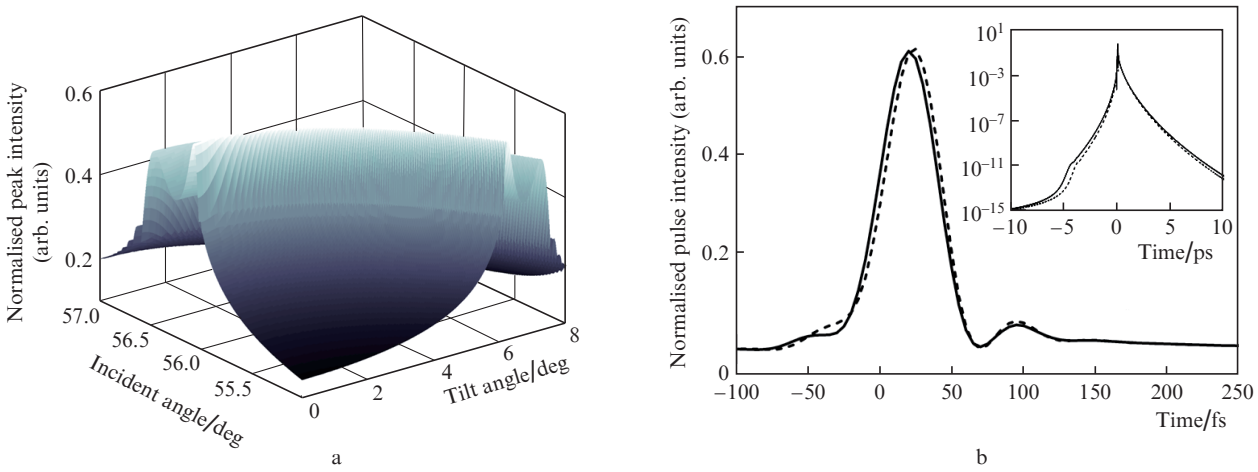

Figure 5. (a) Normalised peak intensity of a GVD compensated pulse as a function of incident angle and out-of-plane tilt angle as well as (b) time dependence of the normalised pulse intensity at (solid curve) $\theta_c = 6.26°$, $\alpha_c = 55°$ and (dashed curve) $\theta_c = 0$, $\alpha_c = 56.07°$. The inset shows the same dependence on an enlarged scale.

Figure 5a shows the peak intensity of the GVD compensated pulse as a function of the incident angle α_c and the out-of-plane tilt angle θ_c. One can see that the highest peak intensity can be obtained by adjusting either the incident angle or the out-of-plane tilt angle. The same quality compressed pulse can be achieved by introducing a 6.26° out-of-plane tilt angle to a compressor with a 55° incident angle (Fig. 5b). In this situation, the nonzero out-of-plane tilt angle at the compressor helps to avoid the amplifier damage caused by the RRP and to compensate for the system dispersion. In most cases, the out-of-plane tilt angles for the RRP suppression and for dispersion compensation are different. In our future multi-petawatt facility, the beam aperture is 250 mm, and the beam path from the final amplifier to the compressor is around 10 m. This means that an out-of-plane tilt angle of 1.5° and an out-of-plane tilt angle of 6.26° are required to suppress the RRP and to compensate for dispersion, respectively; however, at $\theta_c = 6.26°$, both requirements are met. If the 6.26° out-of-plane tilt angle is too large, as shown in Fig. 5a, the highest peak intensity could be maintained by increasing the incident angle and reducing the out-of-plane tilt angle, simultaneously.

Note that in this configuration an increase in the incident angle will not cause the insertion of the second grating into the incident beam. On the contrary, if a very large out-of-plane tilt angle is required to suppress the RRP (as discussed in the previous section), the dispersion compensation problem can be solved by inserting a length-optimised fibre between the grating-stretcher and the amplifier.

4. Conclusions

The RRP is an important problem that determines the actual application of OIGST in an ultra-short, ultra-high, for example petawatt-level, CPA laser system. Slightly tilting the incident beam of the compressor to the grating-groove direction (out-of-plane tilt angle) can prevent the incidence of the RRP into amplifiers, but leads to distortion of dispersion and temporal characteristics of the compressed pulse. Based on our Nd:glass picosecond petawatt laser facility, a useful simple method for TOD compensation is presented, which is based on introducing a length-optimised silica fibre between the stretcher and the amplifier chain and slightly increasing the grating pair distance of the compressor. The simulation result shows that the peak intensity, pulse duration and temporal contrast can be preserved compared to the case when the out-of-plane tilt angle is equal to zero.

In our future Ti:sapphire femtosecond multi-petawatt laser facility, instead of breaking the balance of the system dispersion, the out-of-plane tilt angle of the incident beam at the compressor can be used to compensate for the material dispersion. Apart from solving the RRP problem, the peak intensity and the pulse duration can be improved.

Note that FOD is taken into account in our simulation, but no compensation solution is included. For a higher

requirement, especially <30-fs lasers, a FOD-free method is needed, which will be considered elsewhere.

Acknowledgements. This work was supported by the National Natural Science Foundation of China (Project No. 11304296).

References

1. Yakovlev I.V. *Kvantovaya Elektron*., **44**, 393 (2014) [*Quantum Electron*., **44**, 393 (2014)].
2. Chu Y.-X., Liang X.-Y., Yu L.-H., Xu Y., Xu L., Ma L., Lu X.-M., Liu Y.-Q., Leng Y.-X., et al. *Opt. Express*, **21**, 29231 (2013).
3. Poole P., Trendafilov S., Shvets G., Smith D., Chowdhury E. *Opt. Express*, **21**, 26341 (2013).
4. Li Z.-Y., Xu G., Wang T., Dai Y.-P. *Opt. Lett*., **35**, 2206 (2010).
5. Hein J. Patent DE 10 2008 057 593 A1 (2010).
6. Kessler T.J., Bunkenburg J., Huang H., Kozlov A., Meyerhofer D.D. *Opt. Lett*., **29**, 635 (2004).
7. Cotel A., Castaing M., Pichon P., Le Blanc C. *Opt. Express*, **15**, 2742 (2007).
8. Li Z.-Y., Wang T., Xu G., Li D.-W., Yu J.-W., Ma W.-X., Zhu J., Chen L., Dai Y.-P. *Appl. Opt*., **52**, 718 (2013).
9. Li Z.-Y., Wang T., Xu G., Ouyang X.-P., Li D.-W., Wei H., Yu J.-W., Chen L., Dai Y.-P. *J. Mod. Opt*., **61**, 495 (2014).
10. González Inchauspe C.M., Martínez O.E. *Opt. Lett*., **22**, 1186 (1997).
11. Treacy E.B. *IEEE J. Quantum Electron*., **5**, 454 (1969).
12. Martinez O.E. *IEEE J. Quantum Electron*., **23**, 59 (1987).
13. Cheriaux G., Rousseau P., Salin F., Chambaret J.P., Walker B., Dimauro L.F. *Opt. Lett*., **21**, 414 (1996).
14. Xu G., Wang T., Li Z.-Y., Dai Y.-P., Lin Z.-Q., Gu Y., Zhu J.-Q. *Rev. Laser Eng*., **2008**, 1172 (2008).
15. Kane S., Squier J. *J. Opt. Soc. Am. B*, **14**, 1237 (1997).
16. Zaouter Y., Papadopoulos D.N., Hanna M., Druon F., Cormier E., Georges P. *Opt. Express*, **15**, 9372 (2007).